Molecular Plant Pathology

MOLECULAR PLANT PATHOLOGY (2018) 19(4), 935–947 DOI: 10.1111/mpp.12579

Pseudomonas syringae pv. *tomato* DC3000 polymutants deploying coronatine and two type III effectors produce quantifiable chlorotic spots from individual bacterial colonies in *Nicotiana benthamiana* leaves

SUMA CHAKRAVARTHY[‡,†], JAY N. WORLEY[§,†], ADRIANA MONTES-RODRIGUEZ[¶] AND ALAN COLLMER*

School of Integrative Plant Science, Section of Plant Pathology and Plant-Microbe Biology, Cornell University, Ithaca, NY 14853, USA

SUMMARY

Primary virulence factors of *Pseudomonas syringae* pv. *tomato* DC3000 include the phytotoxin coronatine (COR) and a repertoire of 29 effector proteins injected into plant cells by the type III secretion system (T3SS). DC3000 derivatives differentially producing COR, the T3SS machinery and subsets of key effectors were constructed and assayed in leaves of *Nicotiana benthamiana*. Bacteria were inoculated by the dipping of whole plants and assayed for population growth and the production of chlorotic spots on leaves. The strains fell into three classes. Class I strains are T3SS$^+$ but functionally effectorless, grow poorly *in planta* and produce faint chlorotic spots only if COR$^+$. Class II strains are T3SS$^-$ or, if T3SS$^+$, also produce effectors AvrPtoB and HopM1. Class II strains grow better than class I strains *in planta* and, if COR$^+$, produce robust chlorotic spots. Class III strains are T3SS$^+$ and minimally produce AvrPtoB, HopM1 and three other effectors encoded in the *P. syringae* conserved effector locus. These strains differ from class II strains in growing better *in planta*, and produce chlorotic spots without COR if the precursor coronafacic acid is produced. Assays for chlorotic spot formation, in conjunction with pressure infiltration of low-level inoculum and confocal microscopy of fluorescent protein-labelled bacteria, revealed that single bacteria in the apoplast are capable of producing colonies and associated leaf spots in a 1 : 1 : 1 manner. However, COR makes no significant contribution to the bacterial colonization of the apoplast, but, instead, enables a gratuitous, semi-quantitative, surface indicator of bacterial growth, which is determined by the strain's effector composition.

*Correspondence: Email: arc2@cornell.edu
†These authors contributed equally to this work.
‡Present address: University of Maryland and Food and Drug Administration Joint Institute for Food Safety and Applied Nutrition, College Park, MD 20742, USA.
§Present address: United States Department of Agriculture, Animal and Plant Health Inspection Service, Section of Biotechnology Regulatory Services, Riverdale, MD 20737, USA.
¶Present address: Department of Cell Biology, Friedrich-Alexander University of Erlangen-Nuremberg, Bavaria, Germany.

Keywords: bacterial plant colonization, bacterial polymutants, coronafacic acid, coronatine, effectors, type III secretion system, virulence assays.

INTRODUCTION

Pseudomonas syringae pv. *tomato* (*Pto*) DC3000 is a useful model for unravelling the multifactorial virulence systems that bacteria and other microbes have evolved in the face of the multilayered innate immune systems of higher plants (Xin and He, 2013). *Pto* DC3000 is capable of entering leaves through stomata, growing in the apoplast and producing chlorotic and necrotic disease symptoms in Arabidopsis, tomato and *Nicotiana benthamiana* (if *hopQ1–1* is deleted) (Wei *et al.*, 2007; Xin and He, 2013). These abilities result from the concerted activity of at least two types of virulence factor: multiple effector proteins injected into plant cells via the type III secretion system (T3SS) and the phytotoxin coronatine (COR) (Geng *et al.*, 2014; Lindeberg *et al.*, 2012; Xin and He, 2013).

The study of this virulence system is complicated by the redundancy and interplay amongst and between effectors and COR, and by the presence of multiple functional domains or moieties within effectors and the toxin, respectively. To facilitate the study of individual effectors, we have constructed the nearly effectorless disarmed polymutant DC3000D28E (Cunnac *et al.*, 2011). 'D28E' is deficient in 28 effector genes and has been used previously as a recipient in a gene-shuffling experiment that identified a minimal repertoire of eight effectors for 'D28E+8' to grow to near wild-type levels and produce confluent necrosis when pressure infiltrated into the leaves of *N. benthamiana* (Cunnac *et al.*, 2011).

The subsequent study of D28E and other *Pto* DC3000 mutants yielded additional insights into COR synthesis and effector interplay. First, the unexpected loss of COR production with the deletion of effector gene cluster IX led to the discovery of *cmaL*, which was found to direct the synthesis of L-*allo*-isoleucine, the first step in the biosynthesis of coronamic acid (CMA) (Worley *et al.*, 2013). CMA is conjugated with separately synthesized coronafacic acid

© 2017 BSPP AND JOHN WILEY & SONS LTD

(CFA) in DC3000 to produce the COR holotoxin (Gross and Loper, 2009). Second, D28E retains a weakly expressed gene encoding effector HopAD1, which was found to promote cell death in *N. benthamiana* (at extremely high inoculum levels), unless this activity was suppressed by a previously unknown domain in AvrPtoB, one of the eight effectors in the minimal functional repertoire (Cunnac *et al.*, 2011; Wei *et al.*, 2015). Our ability to restore COR production through the reintegration of *cmaL* into the genome of D28E and derivatives that lack HopAD1 or that express AvrPtoB and small sets of other effectors invited the experiments presented here.

COR is a phytotoxin produced by a subset of *P. syringae* pathovars, including *tomato*, *glycinea*, *maculicola*, *atropurpurea*, *aesculi* and *oryzae* (Baltrus *et al.*, 2011; Gross and Loper, 2009). Its structure, biosynthesis and function have been extensively studied, and it is best described as a multifunctional molecule that targets multiple processes in plant defence (Geng *et al.*, 2014; Xin and He, 2013). COR is a structural and functional mimic of the bioactive isoleucine (Ile) conjugate of jasmonic acid (JA), JA-Ile (Fonseca *et al.*, 2009). The binding of JA-Ile or COR to the F-box protein Coronatine Insensitive 1 (COI1) leads to proteasome-mediated degradation of jasmonate ZIM domain proteins and derepression of JA-responsive genes (Sheard *et al.*, 2010). COR/*COI1*-dependent suppression of salicylic acid accumulation reduces resistance to *Pto* DC3000 in Arabidopsis and tomato (Geng *et al.*, 2012; Uppalapati *et al.*, 2007; Zheng *et al.*, 2012). Other *COI1*-dependent effects of COR in Arabidopsis include the reversal of flagellin-induced stomatal closure (thus enhancing bacterial entry into leaves) and chlorosis, which COR promotes by increasing the expression of the Staygreen/Non-Yellowing/Mendel's 1 locus (SGR) protein that promotes chlorophyll degradation (Bender *et al.*, 1999; Mecey *et al.*, 2011; Melotto *et al.*, 2006; Uppalapati *et al.*, 2005).

COR also has functions that are independent of *COI1*: for example, the stimulation of ethylene (ET) production (Ferguson and Mitchell, 1985; Geng *et al.*, 2014; Uppalapati *et al.*, 2005). ET contributes to the elicitation of cell death associated with bacterial speck disease of tomato caused by *Pto* strains (Cohn and Martin, 2005; Lund *et al.*, 1998). The CMA moiety of COR is similar to 1-aminocyclopropane-1-carboxylic acid (ACC), the precursor of ET (Brooks *et al.*, 2004); however, CMA does not stimulate ET production, and the mechanism by which COR does so is unclear (Geng *et al.*, 2014).

We have shown previously that inoculation by dipping enables *Pto* DC3000 lacking the HopQ1–1 avirulence determinant to cause discrete lesions in *N. benthamiana* leaves, similar to those observed with bacterial speck of tomato in the field (Wei *et al.*, 2007). We subsequently used higher throughput pressure infiltration (with a blunt syringe) assays for bacterial growth and symptom production in *N. benthamiana* leaves to analyse the impact of the progressive disassembly and partial reassembly of the DC3000 effector gene repertoire. Disassembly revealed the importance of two internally redundant effector groups (REGs), AvrPto/AvrPtoB and HopM1/AvrE1/HopR1 (Kvitko *et al.*, 2009), and reassembly of a functional repertoire began with AvrPtoB and HopM1 as representatives of the two REGs (Cunnac *et al.*, 2011).

Here, we have used D28E derivatives producing different COR moieties, AvrPtoB, HopM1 and small subsets of other DC3000 effectors, together with multiple inoculation methods and bioassays, to further explore the impact of COR and effectors on bacterial interactions with *N. benthamiana*. These experiments demonstrate the utility of COR-induced chlorosis as a gratuitous marker for the performance of individual bacterial colonies in *N. benthamiana* leaves; they corroborate the importance of AvrPtoB and HopM1 in virulence and they establish a natural pathosystem that can be reduced to single bacteria producing single colonies and chlorotic spots for the sensitive study of effector actions and interplay.

RESULTS

Restoration of *cmaL* to D28E derivatives with minimal effector sets reveals that COR promotes a range of symptoms in dip-inoculated *N. benthamiana* leaves

We have reported previously that D28E+8 (*avrPtoB*, *hopM1*, *avrE1*, *hopAA1–1*, *hopN1*, *hopE1*, *hopG1*, *hopAM1*) causes complete necrosis in inoculated *N. benthamiana* leaf zones, 6 days after pressure infiltration at 10^5 colony-forming units (CFU)/mL (Cunnac *et al.*, 2011). In contrast, D28E+5 (*avrPtoB*, *hopM1*, *hopE1*, *hopG1*, *hopAM1–1*) causes substantial chlorosis, and D28E+2 (*avrPtoB* and *hopM1*) is virtually symptomless. Here, we asked whether D28E+8 and related strains could produce discrete, speck disease symptoms if we replaced pressure infiltration with the more natural inoculation method of dipping in a bacterial suspension (requiring the pathogen to enter through stomata), and we asked whether restoration of *cmaL* (and thereby COR production) to this series of strains would impact symptoms.

We used Tn*7*-based genomic integration (Choi *et al.*, 2005) to restore *cmaL* to D28E+2, D28E+5, D28E+8 and D28E+*avrPtoB*+CEL. We chose these derivatives because the first three caused a range of symptoms when pressure-infiltrated into *N. benthamiana* leaves (Cunnac *et al.*, 2011), and the fourth derivative enabled us to further evaluate the role of conserved effector locus (CEL) effectors in symptom production. CEL contains the effector genes *hopM1*, *hopAA1–1*, *avrE1* and *hopN1*, the first three of which are nearly universal amongst *P. syringae* pathovars and have been shown to promote cell death in *N. benthamiana*, tomato and/or yeast (Badel *et al.*, 2003, 2006; Munkvold *et al.*, 2008; Wei *et al.*, 2007). Table 1 contains, for each of these strains,

Table 1 *Pseudomonas syringae* pv. *tomato* (*Pto*) DC3000 derivatives used in this study.

Strain	Description	Abbreviated designation	COR moiety	Source
P. syringae pv. *tomato* DC3000	Wild-type; Rif^R	*Pto* DC3000	COR	Cuppels (1986)
CUCPB5585	DC3000D28E; Rif^R Sp^R	D28E	CFA	Cunnac *et al.* (2011)
CUCPB6077	CUCPB5585::Tn*7-cmaL*-Tc; Rif^R Sp^R Tc^R	D28E+*cmaL*	COR	This study
CUCPB6017	D28E+*avrPtoB*+*shcM-hopM1*; Rif^R Sp^R	D28E+2	CFA	Cunnac *et al.* (2011)
CUCPB6080	CUCPB6017::Tn*7-cmaL*-Tc; Rif^R Sp^R Tc^R	D28E+2+*cmaL*	COR	This study
CUCPB6031	D28E+*avrPtoB*+*shcM-hopM1*+*hopE1*+*hopG1*+*hopAM1–1*, Rif^R Sp^R Km^R	D28E+5	CFA	Cunnac *et al.* (2011)
CUCPB6153	CUCPB6031::Tn*7-cmaL*-Tc; Rif^R Sp^R Km^R Tc^R	D28E+5+*cmaL*	COR	This study
CUCPB6019	D28E+*avrPtoB*+CEL; Rif^R Sp^R	D28E+*avrPtoB*+CEL	CFA	Cunnac *et al.* (2011)
CUCPB6081	CUCPB6019::Tn*7-cmaL*-Tc; Rif^R Sp^R Tc^R	D28E+*avrPtoB*+CEL+*cmaL*	COR	This study
CUCPB6032	D28E+*avrPtoB*+CEL+*hopE1*+*hopG1*+*hopAM1–1*; Rif^R Sp^R Km^R	D28E+8	CFA	Cunnac *et al.* (2011)
CUCPB6083	CUCPB6032::Tn*7-cmaL*-Tc; Rif^R Sp^R Km^R Tc^R	D28E+8+*cmaL*	COR	This study
CUCPB6156	CUCPB6017Δ*cfl-cfa9;* Rif^R Sp^R	D28E+2Δ*cfa*	None	This study
CUCPB6106	CUCPB6032Δ*cfl-cfa9;* Rif^R Sp^R	D28E+8Δ*cfa*	None	This study
CUCPB6163	CUCPB6156::Tn*7-cmaL*-Tc; Rif^R Sp^R Tc^R	D28E+2Δ*cfa*+*cmaL*	CMA	This study
CUCPB6109	DC3000D28EΔ*hopAD1* (D29E); Rif^R Sp^R	D29E	CFA	Wei *et al.* (2015)
CUCPB6161	CUCPB6109::Tn*7-cmaL*-Tc; Rif^R Sp^R Tc^R	D29E+*cmaL*	COR	This study
CUCPB5589	CUCPB5585Δ$hrcQ_B$-*U*::FRTGmR; Rif^R Sp^R Gm^R	D28E T3SS$^-$	CFA	Cunnac *et al.* (2011)
CUCPB6162	CUCPB5589::Tn*7-cmaL*-Tc; Rif^R Sp^R Gm^R Tc^R	D28E T3SS$^-$+*cmaL*	COR	This study
CUCPB5113	DC3000Δ$hrcQ_B$-*U*::ΩSpR; Rif^R Sp^R	DC3000 T3SS$^-$	COR	Badel *et al.* (2006)
CUCPB5570	CUCPB5113Δ*hopQ1–1*Δ*cmaL*::FRTSpR; Rif^R Sp^R	DC3000 T3SS$^-$ Δ*cmaL*	CFA	Worley *et al.* (2013)

CFA, coronafacic acid; CMA, coronamic acid; COR, coronatine.

the reference designation, genotype, abbreviated designation used in this report and the COR moiety that is produced.

Plants were dip inoculated at 10^5 CFU/mL with the indicated strains and photographed at 6 days post-inoculation (dpi). In the absence of *cmaL*, D28E+2 and D28E+5 caused virtually no symptoms, whereas D28E+*avrPtoB*+CEL and D28E+8 produced chlorotic spots (Fig. 1A). Unexpectedly, the restoration of *cmaL* enabled all of these D28E derivatives to produce chlorotic spots in *N. benthamiana* leaves. We quantified the intensity of chlorosis seen in inoculated leaves using the Costanza plugin of ImageJ, an image-processing program (Collins, 2007). Costanza is useful for the quantification of chlorotic symptoms as it has options for quantitative measurements of the size and intensity of spots in an image and allows the user to merge compartments. We merged data from discrete spots and from coalesced, spreading chlorotic areas to quantify the total intensity in different leaf samples (Fig. 1B). The results of the quantitative analysis support the visual observations.

We next asked whether COR could promote the formation of discrete chlorotic spots by strains that variously lacked a functional T3SS and/or active effectors. This question was prompted by previous observations indicating that DC3000 T3SS$^-$ produces diffuse chlorosis following syringe infiltration into *N. benthamiana* leaves and this chlorosis is dependent on *cmaL* and COR (Worley *et al.*, 2013). We also restored *cmaL* to both D28E and D29E because D28E grows less well in *N. benthamiana* than its T3SS$^-$ derivative CUCPB5589 (Cunnac *et al.*, 2011) and D28E harbours a weak avirulence determinant, *hopAD1*, which was deleted to produce D29E (Wei *et al.*, 2015).

The test strains were dip inoculated at 10^5 CFU/mL, and inoculated leaves were photographed at 6 dpi. Remarkably, *cmaL*$^+$ variants of D28E, D29E, D28E T3SS$^-$ and DC3000 T3SS$^-$ all produced discrete chlorotic spots, whereas Δ*cmaL* strains did not (Fig. 1C). The representative leaves showed differences in symptoms that were consistently observed in different plants analysed in two independent experiments and were also seen in inoculated whole plants that were photographed at 7 dpi (Fig. S1, see Supporting Information). Specifically, the two T3SS-deficient strains produced a greater number and larger spots than the two effector-deficient T3SS$^+$ strains; the symptoms produced by the former strains overlapped in intensity with those produced by D28E+2+*cmaL* and symptoms were not observed in the absence of *cmaL*. Importantly, weaker symptoms were correlated with the presence of a functional T3SS rather than with the production of HopAD1 (produced by D28E, but not D29E).

Overall, these observations demonstrate that D28E+8, without *cmaL*, can produce symptoms, even when entering through stomata, and indicate that, among the effectors in D28E+8, the conserved effectors AvrE1 and/or HopAA1–1 are more important in the production of chlorotic spots than the variably distributed

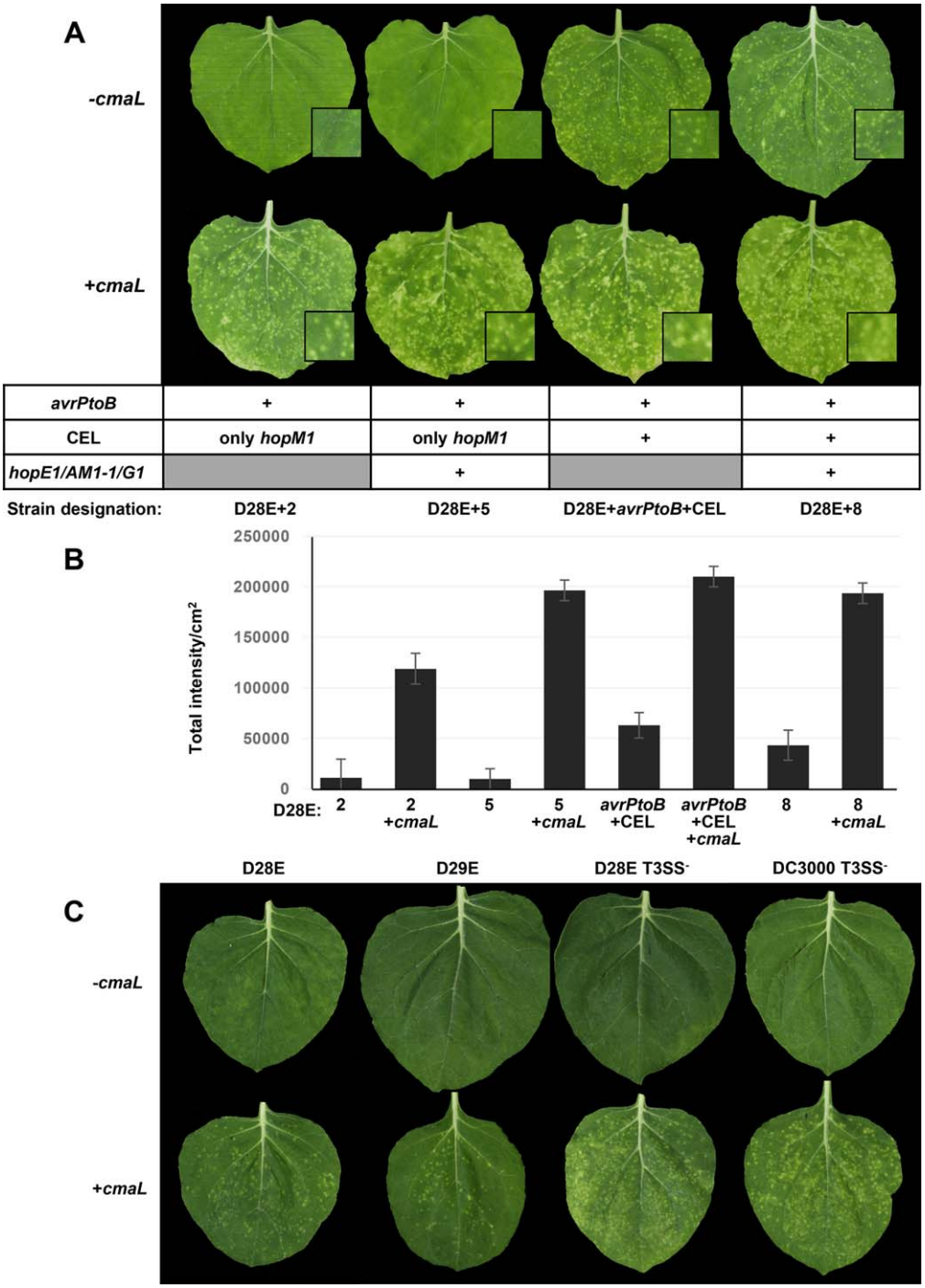

Fig. 1 *Pseudomonas syringae* pv. *tomato* (*Pto*) DC3000 and D28E derivatives with and without *cmaL* reveal the relative contributions of effectors and coronatine (COR) to the production of chlorotic spots in dip-inoculated *Nicotiana benthamiana* leaves. (A) Plants were dip inoculated at 10^5 colony-forming units (CFU)/mL with the indicated strains and photographed at 6 days post-inoculation (dpi). Representative leaves from a single experiment are shown. Three plants were dipped per strain in each experiment and the experiment was repeated three times with similar results. (B) Quantification of the intensity of chlorotic spots corroborates the enhancement of symptom production by *cmaL*. Plants were dip inoculated with the indicated D28E derivatives as described above, and images of 40 leaf samples from two independent experiments were collected at 6 dpi and analysed using ImageJ software. The results represent least-squares means with standard error (SE) of total intensity/cm^2. (C) *Pto* DC3000 and D28E derivatives with and without *cmaL* and a functional type III secretion system (T3SS) reveal that COR is able to promote the production of chlorotic spots in the absence of the T3SS or effectors. Plants were dipped in inoculum of the indicated strains at 10^5 CFU/mL and leaves were photographed at 6 dpi. Three plants were dipped per strain, and representative leaves are shown. The experiment was repeated twice with similar results.

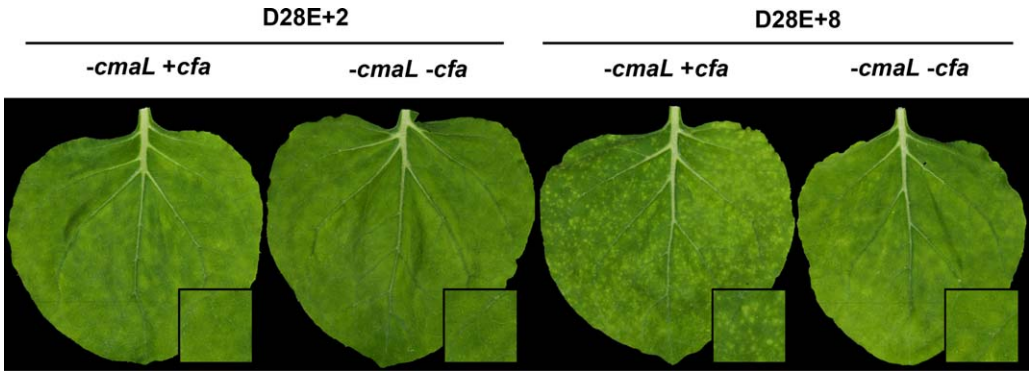

Fig. 2 The discrete chlorotic spots produced by D28E+8 in dip-inoculated *Nicotiana benthamiana* are dependent on coronafacic acid (CFA). D28E+2 and D28E+8 derivatives with and without the *cfa* operon were dip inoculated into *N. benthamiana* leaves at 10^5 CFU/mL, which were then photographed at 6 days post-inoculation (dpi). Three plants were inoculated per strain, and representative leaves are shown. The experiment was repeated twice with similar results.

effectors *hopE1*, *hopG1* and *hopAM1–1*. Remarkably, D28E and D29E can also produce chlorotic spots, albeit faint, if *cmaL* is restored, but D28E+2+*cmaL* produces symptoms that are consistently and notably stronger than those produced by D28E+*cmaL*.

CFA is required for D28E+8 to produce disease symptoms in dip-inoculated *N. benthamiana*

As shown above, D28E+8 can elicit strong chlorosis in *N. benthamiana*. Given that D28E derivatives lacking *cmaL* are expected to accumulate CFA (Worley *et al.*, 2013), we addressed here the potential role of CFA in promoting these symptoms. The polyketide CFA is structurally similar to JA, and exogenous COR, methyl jasmonate (MeJA) and CFA impact partially overlapping transcriptome responses in tomato (Uppalapati *et al.*, 2005). We accordingly deleted the *cfa* biosynthesis operon from D28E+8 and also from D28E+2. Both strains were dip inoculated into *N. benthamiana* at 10^5 CFU/mL, and inoculated leaves were photographed at 6 dpi. As expected, D28E+2 produced only a faint chlorotic mottling without *cmaL*, but the deletion of the *cfa* operon eliminated this subtle effect (Fig. 2). Also as expected, D28E+8 produced strong, discrete chlorotic spots, but, remarkably, these symptoms were eliminated by the deletion of the *cfa* operon, as seen in a representative leaf (Fig. 2) and a whole plant (Fig. S2, see Supporting Information). Thus, the D28E+8 effectors are insufficient to produce chlorotic spot symptoms unless the bacterium also produces either CFA or COR, with COR promoting stronger symptoms than CFA.

CFA, CMA and COR do not contribute significantly to the growth of D28E+2 and D28E+8 in *N. benthamiana*

To determine whether the ability of COR and CFA to promote symptom production by test strains could be attributed to enhanced bacterial growth, we used dipping and pressure infiltration with a blunt syringe to inoculate *N. benthamiana* plants. The inoculum levels in these experiments were 10^5 CFU/mL and 10^4 CFU/mL, respectively, and final population levels were determined by plating at 6 dpi. We observed no significant increase in growth attributable to *cmaL* and COR, regardless of inoculation method (Fig. 3A,B). However, with both inoculation methods, the growth of D28E+2 was significantly higher than that of D28E and, with syringe infiltration, the growth of D28E+8 was significantly higher than that of D28E+2, as observed previously (Cunnac *et al.*, 2011). To assess the potential of CFA to promote growth, we included Δ*cfa* D28E+2 and D28E+8 derivatives in the growth assays, but we observed no significant change in growth regardless of inoculation method.

To determine whether COR conferred a growth advantage that was observable early after dip inoculation, we analysed the growth of D28E+2, with or without *cmaL*, at 1, 2 and 4 dpi (Fig. S3, see Supporting Information). Again, no significant difference was observed amongst the strains tested. Thus, in the D28E/minimal effector–*N. benthamiana* pathosystem, COR has strong effects on disease symptoms without a commensurate effect on bacterial growth *in planta*.

Restoration of *cmaL* to D28E derivatives with minimal effector sets reveals that COR enhances effector-dependent cell death elicitation in *N. benthamiana*

To assess the contribution of COR to cell death elicitation, as indicated by confluent tissue collapse in pressure-infiltrated zones (Cunnac *et al.*, 2011), we analysed three strains with and without *cmaL*. All strains were pressure infiltrated with a blunt syringe at 3×10^6 CFU/mL, and inoculated leaves were photographed 4 days later. As shown in a representative leaf (Fig. 4A), D28E elicited no cell death, even with *cmaL* restored. In contrast, D28E+*avrPtoB*+CEL and D28E+8 both elicited partial collapse of infiltrated zones. Furthermore, with *cmaL* restored, both strains caused confluent collapse. These patterns were also observed

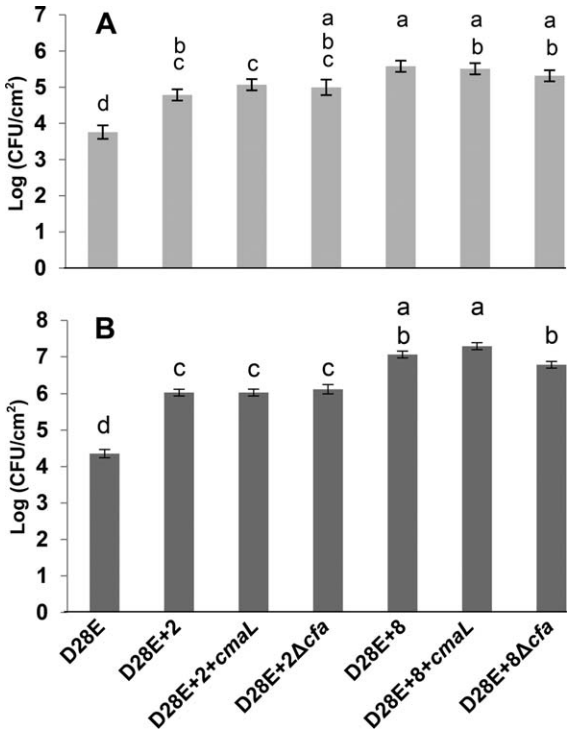

Fig. 3 Coronafacic acid (CFA), coronamic acid (CMA) and coronatine (COR) do not contribute significantly to the growth of D28E+2 or D28E+8 in dip- or syringe-inoculated *Nicotiana benthamiana* leaves. (A) Plants were dipped with the indicated strains at 10^5 colony-forming units (CFU)/mL and bacterial populations in leaf tissue at 6 days post-inoculation (dpi) were determined by plate counting. The chart shows the combined data from five independent experiments, with each experiment containing different subsets of the strains shown. Each strain was evaluated in at least two independent experiments, with three plants per strain in every experiment. (B) Leaves were inoculated by blunt syringe pressure infiltration with the indicated strains at 10^4 CFU/mL, and bacterial populations were measured at 6 dpi. The chart shows combined data from seven independent experiments, with each experiment containing different subsets of the strains shown. Each strain was evaluated in at least three independent experiments, with three plants per strain in every experiment. Growth is depicted as the least-squares means with standard error (SE) of log(CFU/cm^2). Means marked with the same letter are not significantly different using the Tukey honestly significant difference (HSD) method of multiple sample comparison ($\alpha = 0.05$).

with cell death assays based on the measurement of electrolyte leakage from 1.76-cm^2 discs excised from leaves 3 days after syringe infiltration with 1.5×10^6 CFU/mL (Fig. 4B). The restoration of *cmaL* and COR production to D28E+*avrPtoB*+CEL and D28E+8 significantly increased electrolyte leakage. Thus, COR is not sufficient to elicit cell death in the absence of effectors when delivered by pressure infiltration at the above levels of inoculum. In contrast, small sets of effectors that include AvrPtoB and the CEL effectors are sufficient to cause death, but this ability is enhanced by COR.

The symptoms caused by D28E+2+*cmaL* vary from chlorotic spots to confluent necrosis depending on the inoculation technique

We next investigated the effects of different inoculation methods and inoculum levels on symptom production by D28E+2+*cmaL*.

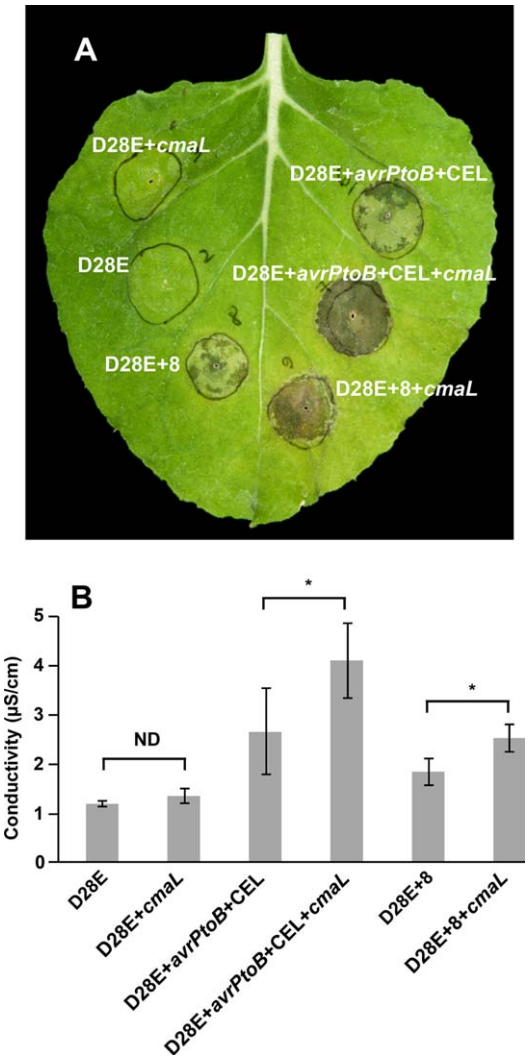

Fig. 4 D28E derivatives carrying small sets of effectors, with and without *cmaL*, reveal relative contributions of effectors and coronatine (COR) to plant cell death and electrolyte leakage in pressure-infiltrated zones in *Nicotiana benthamiana* leaves. (A) D28E+*avrPtoB*+CEL and D28E+8 produce greater cell death in inoculated leaf zones of *N. benthamiana* if *cmaL* is restored to their genome. Leaves were infiltrated with the indicated strains at 10^6 colony-forming units (CFU)/mL and photographed at 4 days post-inoculation (dpi). (B) Restoration of *cmaL* enhances electrolyte leakage from leaf tissue, as assayed by conductivity (µS/cm) of a solution containing leaf discs sampled 3 days after inoculation with D28E+*avrPtoB*+CEL and D28E+8 derivatives at 1.5×10^6 CFU/mL. Each value represents the mean and standard deviation (SD) of four replicates. Pairwise comparisons with asterisks are significantly different ($P < 0.05$); ND, not different. These experiments were repeated twice with similar results.

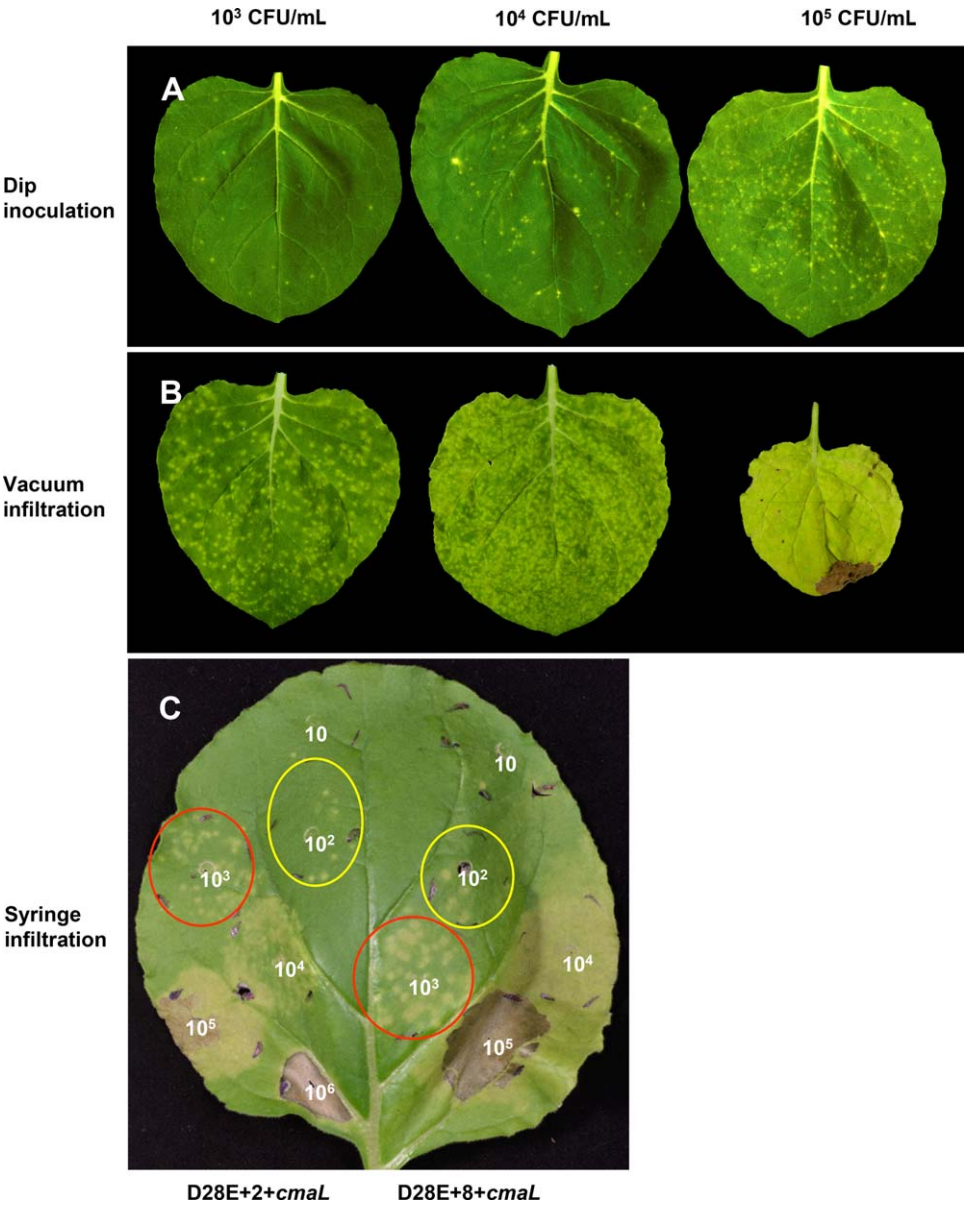

Fig. 5 The method of inoculation and level of inoculum strongly influence the nature of the symptoms produced by D28E+2+*cmaL* and D28E+8+*cmaL* in *Nicotiana benthamiana*. (A, B) Plants were dip inoculated (A) or vacuum infiltrated (B) with D28E+2+*cmaL* at the indicated levels of inoculum, and the plants were photographed at 7 days post-inoculation (dpi) (dip) or 6 dpi (vacuum). Representative leaves from three plants per treatment are shown. It should be noted that all leaves were of equivalent size when inoculated, and similar results were observed in an independent experiment. (C) Zones in *N. benthamiana* leaves were inoculated by syringe infiltration with *c.* 50 μL of bacterial suspension at the indicated colony-forming units (CFU)/mL and photographed at 7 dpi. Black marks on the leaves were used to delineate the perimeter of the infiltration zones, which are further outlined here in red and yellow for inoculations at 10^3 and 10^2 CFU/mL, respectively. Inoculations were similarly performed in three leaves, with a representative leaf shown, and the experiment was repeated twice with similar results.

Plants were inoculated by dipping in 10 mM $MgCl_2$ and 0.04% Silwet L-77 as performed previously (Fig. 1A), but at three different inoculum levels, and photographed at 7 dpi (Fig. 5A). In Fig. 5B, plants were vacuum infiltrated with bacteria in 10 mM $MgCl_2$ and 0.004% Silwet L-77 at the same levels of inoculum as used in Fig. 5A, and photographed at 6 dpi. Consistent with the expectation that bacteria would more efficiently enter the apoplast through stomata with the assistance of vacuum infiltration, inoculum delivered by this method produced symptoms similar to a 100-fold higher level of inoculum delivered by dipping. Notably, D28E+2+*cmaL* vacuum infiltrated at 10^5 CFU/mL inhibited subsequent growth of the leaf and produced some necrosis (Fig. 5B).

We further investigated the relationship between inoculum level and symptom production using a blunt syringe to infiltrate a dilution series of *c.* 50 μL of test bacteria into *N. benthamiana* leaf zones. In addition, we compared the performance of D28E+2+*cmaL* and D28E+8+*cmaL* in producing visible symptoms in this experiment. The starting inoculum for the two strains was normalized on the basis of the optical density at 600 nm (OD_{600}), and serially diluted 10-fold in 10 mM $MgCl_2$. As seen in a representative leaf (Fig. 5C), at high inoculum levels, D28E+2+*cmaL* elicits confluent necrosis, but this response requires *c.* 10-fold more inoculum than with D28E+8+*cmaL*. At intermediate inoculum levels, progressive dilutions produce a shift in symptoms from necrosis to confluent chlorosis and then to

spotty chlorosis, with these transitions occurring at 10-fold higher inoculum levels with D28E+2+*cmaL* relative to D28E+8+*cmaL*. At very low inoculum levels, the two strains produced similar numbers of chlorotic spots. Furthermore, they did so with an efficiency suggesting that the majority of bacteria in a given inoculum can produce a visible spot. The notable difference between the test strains is that spots produced by D28E+8+*cmaL* are larger, which is consistent with the observed larger population levels achieved in syringe-infiltrated *N. benthamiana* leaves by D28E+8 relative to D28E+2 (Cunnac *et al.*, 2011), and by D28E+8+*cmaL* relative to D28E+2+*cmaL* (Fig. 3B). Thus, the chlorotic spots that develop after infiltration of a very low level of bacteria into *N. benthamiana* leaves yield a snapshot approximation of the relative growth of test strains *in planta*.

Measurements of localized bacterial growth and confocal microscopy observations in *N. benthamiana* leaves suggest that single colonies of COR$^+$ bacteria are sufficient to produce individual chlorotic spots

The observations above suggest that, at least at low levels of inoculum, chlorotic spots produced by a COR$^+$ strain may be associated with individual bacterial colonies. This interpretation further suggests that more bacteria will be recovered from chlorotic areas than green areas on leaves inoculated with COR$^+$ strains when these areas are separately sampled. In this regard, it should be noted that, in previously performed growth assays (Fig. 3), we did not bias our sample collection for bacterial enumeration based on symptoms. Our unbiased approach to the sampling of all strains in that experiment was essential because the COR-deficient strains produced no chlorosis to guide targeted sampling. In the present experiment, we exploited COR-dependent chlorosis and used a smaller cork borer (0.13 cm^2 versus the previously used 0.59 cm^2) to excise targeted samples, enabling us to compare bacterial populations in chlorotic spots versus green areas after dip inoculation with D28E+2+*cmaL* at 10^5 CFU/mL. We observed a 2 log increase in the number of bacteria in chlorotic spots relative to green areas (Fig. 6A).

To more directly test the hypothesis that at least some chlorotic spots on a leaf are produced by single bacterial colonies, we labelled D28E+2+*cmaL* with the mCherry fluorescent protein and dip inoculated *N. benthamiana* at 10^5 CFU/mL. At 5 dpi, we marked the perimeters of chlorotic spots on leaves with a black marker and then used confocal microscopy to observe a Z-scan of the delimited areas. We observed in more than four biological repeats that, at this low level of inoculum, a single bacterial colony was often associated with each chlorotic spot, and, as shown in the representative Fig. 6B, the colonies are smaller than the chlorotic spots.

We have shown that restoration of *cmaL* (and therefore COR) does not confer a significant growth benefit to D28E+2 when dip inoculated into *N. benthamiana* leaves (Fig. 3A). To more directly compare the performance *in planta* of D28E+2 with and without COR, we mixed D28E+2+*cmaL* and D28E+2, labelled with

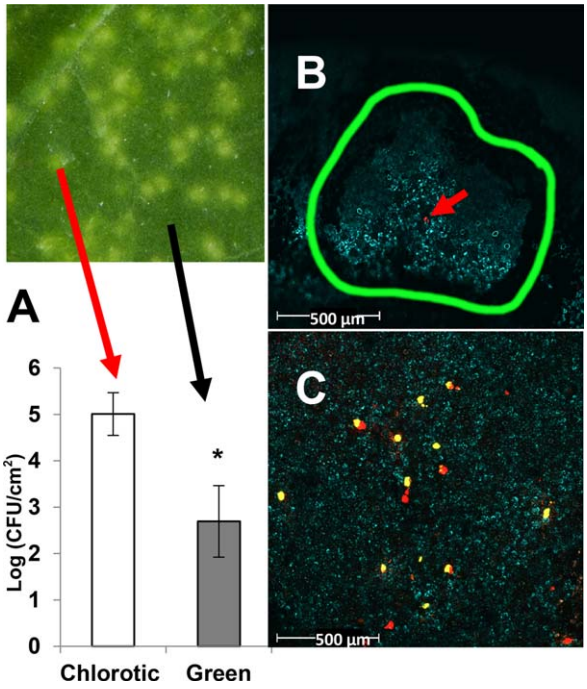

Fig. 6 Measurements of bacterial populations of D28E+2+*cmaL* in chlorotic spots relative to symptomless tissue following dip inoculation, and confocal microscopy of D28E+2 derivatives labelled with fluorescent proteins, indicate that a single coronatine-positive (COR$^+$) bacterial colony can produce a chlorotic spot, but COR has no role in establishing colonies in *Nicotiana benthamiana* leaves. (A) Leaves were dip inoculated with D28E+2+*cmaL* at 10^5 colony-forming units (CFU)/mL, and growth was evaluated in chlorotic leaf spots or green leaf tissue at 6 days post-inoculation (dpi). Growth is depicted as means with standard deviation of log(CFU/cm^2) of 12 leaf discs from three plants per sample. Student's *t*-test was used to evaluate the significance of the difference (*$P \leq 0.001$). The experiment was repeated three times with similar results. The size of the leaf discs used for bacterial enumeration was 0.13 cm^2. (B) D28E+2+*cmaL* labelled with mCherry was used to dip inoculate *N. benthamiana* plants at 10^5 CFU/mL, and confocal microscopy was used to image colony formation in leaves at 5 dpi. Colonies were found to be localized in chlorotic spots, whose perimeters were delineated with a black marker before microscopy (interior border outlined in green). Shown here is a representative image with a single colony (arrow) associated with a chlorotic spot in a confocal cross-section overlay of chlorophyll fluorescence (cyan) and mCherry fluorescence (red). (C) D28E+2+*cmaL* labelled with mCherry was mixed 1 : 1 with D28E+2 labelled with yellow fluorescent protein (YFP), and the mixture was dip inoculated at 10^8 CFU/mL into leaves. Leaf areas were imaged using confocal microscopy at 5 dpi. Both D28E+2+*cmaL* (red colonies) and D28E+2 (yellow colonies) were observed in approximately equal numbers. The representative image shown here is a three-dimensional stack compressed to one plane, and chlorophyll fluorescence is shown in grey. Additional images from four independent experiments are shown in Fig. S4 (see Supporting Information).

mCherry and yellow fluorescent protein (YFP), respectively, and dip inoculated *N. benthamiana* at 10^8 CFU/mL. Confocal microscopy of random leaf areas (without reference to chlorotic symptoms) revealed approximately equal numbers of D28E+2+*cmaL* and D28E+2 colonies (Fig. 6C; see Fig. S4, Supporting Information, for more images). These results support our conclusion that COR strongly affects the symptoms produced by D28E+2 without a commensurate impact on colony formation or total growth in *N. benthamiana*.

DISCUSSION

We have used derivatives of the disarmed polymutant D28E to investigate the interplay of COR moieties, the T3SS and key type III effectors in the production of phenotypic readouts for bacterial infection in the model plant *N. benthamiana*. An unexpected finding is that, in common laboratory conditions, COR makes no discernible contribution to the colonization or growth of D28E derivatives in *N. benthamiana* leaves, regardless of inoculation method. However, COR (or CFA in some cases) is essential for the chlorosis that attends growth. Thus, the primary impact of the restoration of *cmaL* to D28E is to enable the relative success of bacteria *in planta* to be semi-quantitatively displayed on the leaf surface in the form of chlorotic spots that mimic field symptoms.

Our conclusion that individual D28E+2+*cmaL* cells can efficiently establish single colonies in *N. benthamiana*, which then produce single chlorotic spots, is supported by experiments with low-dose inoculum and by confocal microscopy. Importantly, chlorotic spots of similar appearance are produced by D28E+2+*cmaL* with three different inoculation methods if the inoculum levels are adjusted to deliver equivalent numbers of bacteria into the leaf. Thus, semi-quantitative assessment of interactions between D28E derivatives and *N. benthamiana* (and potential immune system variants) based on the density and size of chlorotic spots can be achieved simply by using extremely low doses of bacteria in pressure infiltrations.

It is important to note that D28E+2+*cmaL* does not elicit effector-triggered immunity (ETI)-associated hypersensitive cell death. In contrast, a landmark early study of *P. syringae–Nicotiana tabacum* interactions used serial dilutions of an ETI-eliciting avirulent strain to reveal that individual bacterial cells trigger the death of individual leaf mesophyll cells in a 1 : 1 manner (Turner and Novacky, 1974) (a phenomenon we now see as mechanistically based on the contact-dependent delivery of effectors by the T3SS). Thus, high inoculum levels of avirulent bacteria (typically 10^7 CFU/mL) are needed for sufficient individual mesophyll cell deaths to manifest in macroscopically visible tissue collapse in infiltrated zones. In contrast, we have found that even weakly virulent COR^+ D28E derivatives in *N. benthamiana* are capable of 1 : 1 : 1 (bacterium > colony > chlorotic spot) interactions that produce symptoms with remarkably few input bacteria.

Pseudomonas syringae can have various alternative interactions with plants (Hirano and Upper, 1990). For example, toothpick wound inoculations revealed a potential for limited spread of *Pto* DC3000 through *N. benthamiana* xylem vessels (Misas-Villamil *et al.*, 2011), and early studies of *P. syringae* with mixed infections at higher levels of inoculum showed a general potential for both cooperativity and interference within the leaves of various plants. That is, compatible (virulent) strains of *P. syringae* promote the growth of non-pathogens or $T3SS^-$ mutants, whereas incompatible (ETI-eliciting) strains inhibit the growth of compatible strains (Hirano *et al.*, 1999; Klement and Lovrekovich, 1961; Young, 1974). Recently, these patterns have been confirmed and extended through confocal microscopy of bean leaves inoculated with mixtures of fluorescent protein-labelled *P. syringae* virulence variants (Rufian *et al.*, 2017). Confocal microscopy observations also suggest that bacteria concentrating at leaf entry points contribute to the formation of the spot symptoms characteristic of many *P. syringae* diseases (Boureau *et al.*, 2002; Rufian *et al.*, 2017).

Mixed infections with *P. syringae* strains are also used in competitive index assays, which have been shown to detect differences in growth potential with greater statistical discrimination, in part because the growth of control and test bacteria in the same tissue eliminates plant-to-plant variation (Macho *et al.*, 2007). Importantly, such assays rely on the use of empirically determined levels of inoculum (typically 5×10^4 CFU/mL) that are low enough for the pressure-infiltrated strains being compared not to affect each other's growth (Macho *et al.*, 2007).

In comparison with assays based on dip inoculation, vacuum infiltration and competitive indexing, the low-dose pressure infiltration chlorotic spot assay offers several advantages that are particularly useful for the study of interactions of *P. syringae* with large-leaved *Nicotiana* spp. (i) Relative to dip inoculation or vacuum infiltration, syringe infiltration enables more precise control of the numbers of bacteria delivered, and better control of inoculum and spot density can facilitate studies of the development of individual bacterial colonies and spatial aspects of plant responses within a leaf. (ii) The ability to make several inoculations on each of several leaves reduces the problem of plant-to-plant variation and facilitates the use of internal controls. (iii) Because of the visual nature of the readout (in contrast with competitive index growth assays), screening for pathogen or plant genes with disease interaction phenotypes should be amenable to new high-throughput imaging tools (Fahlgren *et al.*, 2015; Mutka *et al.*, 2016). Recently, ImageJ has been used to quantify total chlorosis in flats of Arabidopsis spray inoculated with *P. syringae*, and to thereby demonstrate a correlation between chlorosis and bacterial growth (Laflamme *et al.* 2016). As demonstrated here, comparisons of chlorotic spot symptoms in relation to bacterial genotype were key to our evaluation of the role of COR.

Table 2 Three classes of *Pseudomonas syringae* pv. *tomato* (*Pto*) DC3000 derivative defined by growth and chlorotic spot phenotypes in *Nicotiana benthamiana* leaves.

Class	Key features of strains in class	Relative growth	Chlorotic spots if COR$^-$ and CFA$^+$	Chlorotic spots if COR$^+$
I	T3SS$^+$ but functionally effectorless	1	No	Yes, faint
II	T3SS$^-$ (regardless of effector repertoire) or D28E/D29E/D36E+2*	2	No	Yes, robust
III	D28E+8 or D28E+AvrPtoB+CEL	3	Yes	Yes, larger than class II COR$^+$ and class III CFA$^+$

*+2 denotes AvrPtoB+HopM1; +8 denotes AvrPtoB+CEL+HopE1+HopG1+HopAM1.

Our findings with *cmaL*-restored strains revealed significant differences in the contributions of COR to the *Pto* DC3000 infection process in *N. benthamiana* and those reported for Arabidopsis, where the major impact of COR is in the promotion of bacterial entry to the leaf apoplast via stomata (Melotto *et al.*, 2006, 2008; Zeng *et al.*, 2011). We saw no evidence of such a requirement with *N. benthamiana* in our dip inoculation experiments. We postulate that the use of inoculum containing Silwet L-77 with plants that are conditioned overnight in a humid chamber obviates any need for COR in bacterial entry in *N. benthamiana*, but we did not use alternative humidity, inoculum levels or other experimental variables to explore this further. It is also noteworthy that *P. syringae* pv. *tabaci*, which causes wildfire disease of tobacco and other *Nicotiana* spp. in the field, does not produce COR (Hwang *et al.*, 2005; Studholme *et al.*, 2009). In Arabidopsis, COR can contribute to the growth of *Pto* DC3000 following direct infiltration into the leaf apoplast, but this effect is not observed with higher levels of inoculum, for example, 10^6 CFU/mL rather than 10^5 CFU/mL (Brooks *et al.*, 2004; Geng *et al.*, 2012; Melotto *et al.*, 2006; Mittal and Davis, 1995; Zeng and He, 2010). In contrast, we observed that the multiplication of D28E derivatives delivered at very low levels into *N. benthamiana* leaves was unaffected by the production of either CFA or COR.

The ability of COR-mediated chlorosis to serve as a gratuitous marker for the colony development of disarmed DC3000 derivatives in *N. benthamiana* should aid the analysis of certain effectors, particularly those that overlap with COR in targeting ET and JA signalling (Geng *et al.*, 2014). The problem of redundancy between effectors and COR in interaction phenotypes has already been observed with *Pto* DC3000 in Arabidopsis and tomato infections: COR and the CEL effectors make partially redundant contributions to the growth of DC3000 in Arabidopsis leaves (Geng *et al.*, 2012), and the CEL effector HopAA1–1 and COR function redundantly in promoting lesions in dip-inoculated tomato (Munkvold *et al.*, 2009).

Our observations of chlorotic spot symptoms corroborate assays of bulk growth and confluent symptoms in defining three classes of disarmed DC3000 mutants that consistently differ in their rank order performance in *N. benthamiana* leaves (Table 2). Class I strains, such as D28E, show nearly two logs less growth than T3SS-deficient mutants of D28E and DC3000 (Cunnac *et al.*, 2011), and our findings here provide more evidence that this reduced growth results from the T3SS machinery rather than any residual effectors functioning as weak avirulence determinants. Class II strains include both T3SS$^-$ DC3000 and D28E+2+*cmaL*, with the latter strain possibly suppressing T3SS machinery-dependent defence through the action of AvrPtoB (Wei *et al.*, 2015).

D28E derivatives in class III (D28E+8 and D28E+AvrPtoB+CEL) have the defining property of eliciting chlorotic spots when producing only CFA rather than the more biologically active COR holotoxin. Class III strains also cause significant necrosis when pressure infiltrated and sometimes when dip inoculated, and they grow significantly better than class II strains following pressure infiltration. Intriguingly, our data indicate that the impact of effectors on *Pto* DC3000 performance in *N. benthamiana* is to prolong the growth of bacterial colonies, but the colonies are initially established in an effector-independent manner. Finally, it is important to note that class III strains are less virulent with regard to growth or symptoms than *Pto* DC3000Δ*hopQ1–1* (Cunnac *et al.*, 2011).

The remarkable ability of COR$^+$ D28E expressing only HopM1 and AvrPtoB to produce robust chlorotic spot symptoms in *N. benthamiana* leaves provides additional support for a new model for *P. syringae* pathogenesis, which proposes that effector repertoires perform two primary functions: apoplast watersoaking and pathogen-associated molecular pattern (PAMP)-triggered immunity (PTI) suppression (Xin *et al.*, 2016). Notably, HopM1 was found to promote watersoaking in a manner dependent on its previously shown ability to destroy the Arabidopsis AtMIN7 ADP ribosylation factor–guanine nucleotide exchange factor protein involved in vesicle trafficking (Nomura *et al.*, 2006; Xin *et al.*, 2016).

The experimental pathosystem involving disarmed DC3000 derivatives and *N. benthamiana* offers many advantages for exploring the contribution of individual effectors to disease development. Individual effectors can be studied in the context of pathogen–host interactions that involve the native delivery of

pathogen factors and natural readouts for disease processes, including bacterial growth and the formation of the chlorotic and necrotic lesions that are characteristic of bacterial speck disease. The importance of using native delivery has been demonstrated recently through the discovery of domains in AvrPtoB that quantitatively interfere with each other in their modes of ETI suppression (Wei *et al.*, 2015). The advantages of *N. benthamiana* as a host to be probed for pathogen virulence and plant immunity factors include its ease of inoculation by dipping, vacuum infiltration and, especially, blunt syringe infiltration, amenability to virus-induced gene silencing and a growing set of genomic resources (Bombarely *et al.*, 2012; Goodin *et al.*, 2008) (http://bti.cornell.edu/research/projects/nicotiana-benthamiana). Finally, we have shown that functionally effectorless *Pto* DC3000 derivatives that have been restored for the production of COR and two key effectors, HopM1 and AvrPtoB, produce chlorotic spots at a seemingly optimum level for the identification of additional pathogen and plant factors that either promote or reduce disease.

EXPERIMENTAL PROCEDURES

Bacterial strains and plasmids

The *Pto* DC3000 derivatives used in this study are listed in Table 1. *Escherichia coli* strains and plasmids used in strain constructions are listed in Table S1, Table S2, Method S1 (see Supporting Information). *Escherichia coli* DH5α was used for general cloning procedures. In addition, *E. coli* DB3.1 was used for the propagation of Gateway plasmids containing the lethal *ccdB* gene. *Escherichia coli* strains were grown in Luria–Bertani (LB) broth at 37 °C. *Pto* DC3000 derivatives were grown in King's B (KB) medium at 28 °C. Antibiotics were used at the following final concentrations (μg/mL): ampicillin (Ap), 100; kanamycin (Km), 50; gentamicin (Gm), 10; spectinomycin (Sp), 50; rifampicin (Rf), 50; tetracycline (Tc), 10; chloramphenicol (Cm), 20.

Preparation of bacteria for plant inoculations

Pseudomonas strains were grown from frozen stocks on KB agar medium containing appropriate antibiotics. One day prior to plant inoculation, small amounts of bacteria were scraped off the plate, resuspended in 100–200 μL of 10 mM $MgCl_2$, spotted onto fresh plates and grown for a day. Cells were harvested the following day and OD_{600} was measured. The cells were adjusted to an OD_{600} of 0.3 in 10 mM $MgCl_2$, equivalent to 3×10^8 CFU/mL under our conditions, and then diluted in 10 mM $MgCl_2$ to achieve the desired final concentration for plant inoculation.

Plant inoculations and bacterial growth assays

Six-week-old *N. benthamiana* plants were grown in a glasshouse and transferred to the laboratory 2–3 days prior to inoculation with bacterial strains. For dip inoculations, well-watered plants were arranged on a tray and covered with a large bag in order to create a humid chamber, and left overnight on the laboratory bench. Each plant was removed from the bag immediately prior to dipping. Plants were dipped in a bacterial suspension at 10^5 CFU/mL in 10 mM $MgCl_2$ with 0.04% Silwet L-77 for 1 min each. After inoculation, plants were allowed to air dry and then transferred to a growth chamber at 24–25 °C, ≥70% relative humidity (RH) and 16 h day length. For vacuum infiltration, 4-week-old plants were vacuum infiltrated with a bacterial suspension at 10^3–10^5 CFU/mL in 10 mM $MgCl_2$ with 0.004% Silwet L-77. Plants were allowed to air dry and then transferred to the plant chamber. For syringe inoculation, bacteria were suspended at a final concentration ranging from 3×10^2 to 3×10^7 CFU/mL in 10 mM $MgCl_2$, and infiltrated with a 1-mL blunt syringe into well-expanded leaves. After the development of symptoms, leaves were removed and photographed.

For growth assays, bacterial populations were measured at 6 dpi unless noted otherwise. Three 0.59-cm^2 leaf discs (except as noted for Fig. 6) were harvested with a cork borer from dip-inoculated leaves or from marked, syringe-infiltrated leaf zones and ground in 10 mM $MgCl_2$. Leaf extracts were serially diluted in 10 mM $MgCl_2$ and spotted onto KB agar medium with antibiotics. Bacterial colonies were counted and expressed as CFU/cm^2. An unbalanced block design with random effects of experiment or experiment × strain was used for statistical analysis of the data using the program JMP Pro11. Tukey's honestly significant difference (HSD) method was used to determine the significance of growth differences between strains ($\alpha = 0.05$).

Quantitative analysis of leaf chlorosis

JPG files of leaf images were analysed using ImageJ, an image-processing program available in the public domain. The area of each leaf was measured as described in the link http://rsb.info.nih.gov/ij/docs/pdfs/examples.pdf. The intensity of chlorotic symptoms on the leaves was quantified using the Costanza plugin in ImageJ (http://home.thep.lu.se/~henrik/Costanza/). Briefly, the mid-rib portion of the leaf was first removed from the images to minimize the background signal. The configuration and parameters used for image analysis are shown in Fig. S5 (see Supporting Information). Results for each image were saved in an Excel file. The intensity of each cell (or chlorotic spot) was calculated by multiplying the basin of attraction (BOA) volume by the mean cell intensity, and the intensities of all the cells in an image were added to yield the total intensity. Symptoms were depicted as total intensity/cm^2 of leaf area.

Electrolyte leakage assay

Quantification of cell death was performed by measurement of the electrolyte leakage at 3 days after syringe infiltration with the indicated bacterial mutant strains at 1.5×10^6 CFU/mL (Cook and Stall, 1968; López-Solanilla *et al.*, 2004). For electrolyte leakage experiments, three leaf discs of 1.76 cm^2 were placed into a 50-mL conical centrifuge tube with 25 mL of deionized water. After 40 min of incubation on a rotary shaker at room temperature, the conductivity was determined using a Mettler-Toledo CompactSeven pH/Ion S220 Instrument (Columbus, OH, USA).

Confocal microscopy

Images were captured on a Leica TCS SP5 confocal microscope (Buffalo Grove, IL, USA). YFP fluorescence was captured with excitation at 514 nm and emission from 524 to 549 nm. mCherry fluorescence was captured with excitation at 561 nm and emission from 593 to 618 nm. Transmitted

light was captured using a 561-nm laser. Images were captured using sequential scanning for the different fluorescent proteins with 2× line averaging to improve image accuracy. Images were captured from the top of the leaf for viewing individual spots at 10^5 CFU/mL and from the bottom for viewing mixtures at 10^8 CFU/mL. Confocal image adjustments and focal plane Z-scans were combined using the software program LAS AF Lite 2.6.0 (Leica Microsystems, Buffalo Grove, IL, USA).

ACKNOWLEDGEMENTS

We thank Claire Smith and Kent Loeffler for photography, Lynn Johnson (Cornell Statistical Consulting Unit) for help with data analysis, Cecillia Leeand for technical assistance, Hai-Lei Wei for construction of CUCPB6106, Adrienne Roeder (Plant Biology Section) for help with the quantitative analysis of symptoms, and Mamta Srivastava and the Boyce Thompson Institute for the use of their Plant Cell Imaging Center. This work was funded by United States National Science Foundation grant IOS-1025642. Adriana Montes-Rodriguez was supported by German Research Council (Deutsche Forschungsgemeinschaft) Collaborative Research Center 796, project C7. The authors have no conflicts of interest to declare.

REFERENCES

Badel, J.L., Nomura, K., Bandyopadhyay, S., Shimizu, R., Collmer, A. and He, S.Y. (2003) *Pseudomonas syringae* pv. *tomato* DC3000 HopPtoM (CEL ORF3) is important for lesion formation but not growth in tomato and is secreted and translocated by the Hrp type III secretion system in a chaperone-dependent manner. *Mol. Microbiol.* **49**, 1239–1251.

Badel, J.L., Shimizu, R., Oh, H.-S. and Collmer, A. (2006) A *Pseudomonas syringae* pv. *tomato avrE1*/*hopM1* mutant is severely reduced in growth and lesion formation in tomato. *Mol. Plant–Microbe Interact.* **19**, 99–111.

Baltrus, D.A., Nishimura, M.T., Romanchuk, A., Chang, J.H., Mukhtar, M.S., Cherkis, K., Roach, J., Grant, S.R., Jones, C.D. and Dangl, J.L. (2011) Dynamic evolution of pathogenicity revealed by sequencing and comparative genomics of 19 *Pseudomonas syringae* isolates. *PLoS Pathog.* **7**, e1002132.

Bender, C.L., Alarcon-Chaidez, F. and Gross, D.C. (1999) *Pseudomonas syringae* phytotoxins: mode of action, regulation, and biosynthesis by peptide and polyketide synthetases. *Microbiol. Mol. Biol. Rev.* **63**, 266–292.

Bombarely, A., Rosli, H.G., Vrebalov, J., Moffett, P., Mueller, L.A. and Martin, G.B. (2012) A draft genome sequence of *Nicotiana benthamiana* to enhance molecular plant–microbe biology research. *Mol. Plant–Microbe Interact.* **12**, 1523–1530.

Boureau, T., Routtu, J., Roine, E., Taira, S. and Romantschuk, M. (2002) Localization of *hrpA*-induced *Pseudomonas syringae* pv. *tomato* DC3000 in infected tomato leaves. *Mol. Plant Pathol.* **3**, 451–460.

Brooks, D., Hernandez-Guzman, G., Koek, A.P., Alarcon-Chaidez, F., Sreedharan, A., Rangaswarmy, V., Penaloza-Vasquez, A., Bender, C.L. and Kunkel, B.N. (2004) Identification and characterization of a well-defined series of coronatine biosynthetic mutants of *Pseudomonas syringae* pv. *tomato* DC3000. *Mol. Plant–Microbe Interact.* **17**, 162–174.

Choi, K.H., Gaynor, J.B., White, K.G., Lopez, C., Bosio, C.M., Karkhoff-Schweizer, R.R. and Schweizer, H.P. (2005) A Tn7-based broad-range bacterial cloning and expression system. *Nat. Methods*, **2**, 443–448.

Cohn, J.R. and Martin, G.B. (2005) *Pseudomonas syringae* pv. *tomato* type III effectors AvrPto and AvrPtoB promote ethylene-dependent cell death in tomato. *Plant J.* **44**, 139–154.

Collins, T.J. (2007) ImageJ for microscopy. *Biotechniques*, **43**, 25–30.

Cook, A.A. and Stall, R.E. (1968) Effect of *Xanthomonas vesicatoria* on loss of electrolytes from leaves of *Capsicum annum*. *Phytopathology*, **58**, 617–619.

Cunnac, S., Chakravarthy, S., Kvitko, B.H., Russell, A.B., Martin, G.B. and Collmer, A. (2011) Genetic disassembly and combinatorial reassembly identify a minimal functional repertoire of type III effectors in *Pseudomonas syringae*. *Proc. Natl. Acad. Sci. USA*, **108**, 2975–2980.

Cuppels, D.A. (1986) Generation and characterization of Tn*5* insertion mutations in *Pseudomonas syringae* pv. *tomato*. *Appl. Environ. Microbiol.* **51**, 323–327.

Fahlgren, N., Gehan, M.A. and Baxter, I. (2015) Lights, camera, action: high-throughput plant phenotyping is ready for a close-up. *Curr. Opin. Plant Biol.* **24**, 93–99.

Ferguson, I.B. and Mitchell, R.E. (1985) Stimulation of ethylene production in bean leaf discs by the pseudomonad phytotoxin coronatine. *Plant Physiol.* **77**, 969–973.

Fonseca, S., Chini, A., Hamberg, M., Adie, B., Porzel, A., Kramell, R., Miersch, O., Wasternack, C. and Solano, R. (2009) (+)-7-iso-Jasmonoyl-L-isoleucine is the endogenous bioactive jasmonate. *Nat. Chem. Biol.* **5**, 344–350.

Geng, X., Cheng, J., Gangadharan, A. and Mackey, D. (2012) The coronatine toxin of *Pseudomonas syringae* is a multifunctional suppressor of *Arabidopsis* defense. *Plant Cell*, **24**, 4763–4774.

Geng, X., Jin, L., Shimada, M., Kim, M.G. and Mackey, D. (2014) The phytotoxin coronatine is a multifunctional component of the virulence armament of *Pseudomonas syringae*. *Planta*, **240**, 1149–1165.

Goodin, M.M., Zaitlin, D., Naidu, R.A. and Lommel, S.A. (2008) *Nicotiana benthamiana*: its history and future as a model for plant–pathogen interactions. *Mol. Plant–Microbe Interact.* **21**, 1015–1026.

Gross, H. and Loper, J.E. (2009) Genomics of secondary metabolite production by *Pseudomonas* spp. *Nat. Prod. Rep.* **26**, 1408–1446.

Hirano, S.S. and Upper, C.D. (1990) Population biology and epidemiology of *Pseudomonas syringae*. *Annu. Rev. Phytopathol.* **28**, 155–177.

Hirano, S., Charkowski, A.O., Collmer, A., Willis, D.K. and Upper, C.D. (1999) Role of the Hrp type III protein secretion system in growth of *Pseudomonas syringae* pv. *syringae* B728a on host plants in the field. *Proc. Natl. Acad. Sci. USA*, **96**, 9851–9856.

Hwang, M.S., Morgan, R.L., Sarkar, S.F., Wang, P.W. and Guttman, D.S. (2005) Phylogenetic characterization of virulence and resistance phenotypes of *Pseudomonas syringae*. *Appl. Environ. Microbiol.* **71**, 5182–5191.

Klement, Z. and Lovrekovich, L. (1961) Defense reactions induced by phytopathogenic bacteria in bean pods. *Phytopathol. Z.* **41**, 217–227.

Kvitko, B.H., Park, D.H., Velásquez, A.C., Wei, C.-F., Russell, A.B., Martin, G.B., Schneider, D.J. and Collmer, A. (2009) Deletions in the repertoire of *Pseudomonas syringae* pv. *tomato* DC3000 type III secretion effector genes reveal functional overlap among effectors. *PLoS Pathog.* **5**, e1000388.

Laflamme, B., Middleton, M., Lo, T., Desveaux, D. and Guttman, D.S. (2016) Image-based quantification of plant immunity and disease. *Mol. Plant–Microbe Interact.* **29**, 919–924.

Lindeberg, M., Cunnac, S. and Collmer, A. (2012) *Pseudomonas syringae* type III effector repertoires: last words in endless arguments. *Trends Microbiol.* **20**, 199–208.

López-Solanilla, E., Bronstein, P.A., Schneider, A.R. and Collmer, A. (2004) HopPtoN is a *Pseudomonas syringae* Hrp (type III secretion system) cysteine protease effector that suppresses pathogen-induced necrosis associated with both compatible and incompatible plant interactions. *Mol. Microbiol.* **54**, 353–365.

Lund, S.T., Stall, R.E. and Klee, H.J. (1998) Ethylene regulates the susceptible response to pathogen infection in tomato. *Plant Cell*, **10**, 371–382.

Macho, A.P., Zumaquero, A., Ortiz-Martin, I. and Beuzón, C.R. (2007) Competitive index in mixed infections: a sensitive and accurate assay for the genetic analysis of *Pseudomonas syringae*–plant interactions. *Mol. Plant Pathol.* **8**, 437–450.

Mecey, C., Hauck, P., Trapp, M., Pumplin, N., Plovanich, A., Yao, J. and He, S.Y. (2011) A critical role of *STAYGREEN*/Mendel's I locus in controlling disease symptom development during *Pseudomonas syringae* pv *tomato* infection of Arabidopsis. *Plant Physiol.* **157**, 1965–1974.

Melotto, M., Underwood, W., Koczan, J., Nomura, K. and He, S.Y. (2006) Plant stomata function in innate immunity against bacterial invasion. *Cell*, **126**, 969–980.

Melotto, M., Underwood, W. and He, S.Y. (2008) Role of stomata in plant innate immunity and foliar bacterial diseases. *Annu. Rev. Phytopathol.* **46**, 101–122.

Misas-Villamil, J.C., Kolodziejek, I. and Van Der Hoorn, R.A. (2011) *Pseudomonas syringae* colonizes distant tissues in *Nicotiana benthamiana* through xylem vessels. *Plant J.* **67**, 774–782.

Mittal, S. and Davis, K.R. (1995) Role of the phytotoxin coronatine in the infection of *Arabidopsis thaliana* by *Pseudomonas syringae* pv. *tomato*. *Mol. Plant–Microbe Interact.* **8**, 165–171.

Munkvold, K.R., Martin, M.E., Bronstein, P.A. and Collmer, A. (2008) A survey of the *Pseudomonas syringae* pv. *tomato* DC3000 type III secretion system effector repertoire reveals several effectors that are deleterious when expressed in *Saccharomyces cerevisiae*. *Mol. Plant–Microbe Interact.* **21**, 490–502.

Munkvold, K.R., Russell, A.B., Kvitko, B.H. and Collmer, A. (2009) *Pseudomonas syringae* pv. *tomato* DC3000 type III effector HopAA1–1 functions redundantly

with chlorosis-promoting factor PSPTO4723 to produce bacterial speck lesions in host tomato. *Mol. Plant–Microbe Interact.* **22**, 1341–1355.

Mutka, A.M., Fentress, S.J., Sher, J.W., Berry, J.C., Pretz, C., Nusinow, D.A. and Bart, R. (2016) Quantitative, image-based phenotyping methods provide insight into spatial and temporal dimensions of plant disease. *Plant Physiol.* **172**, 650–660.

Nomura, K., Debroy, S., Lee, Y.H., Pumplin, N., Jones, J. and He, S.Y. (2006) A bacterial virulence protein suppresses host innate immunity to cause plant disease. *Science*, **313**, 220–223.

Rufian, J.S., Macho, A.P., Corry, D.S., Mansfield, J., Ruiz-Albert, J., Arnold, D. and Beuzon, C.R. (in press) Confocal microscopy reveals *in planta* dynamic interactions between pathogenic, avirulent and non-pathogenic *Pseudomonas syringae* strains. *Mol. Plant Pathol.* doi 10.1111/mpp.12539.

Sheard, L.B., Tan, X., Mao, H., Withers, J., Ben-Nissan, G., Hinds, T.R., Kobayashi, Y., Hsu, F.F., Sharon, M., Browse, J., He, S.Y., Rizo, J., Howe, G.A. and Zheng, N. (2010) Jasmonate perception by inositol-phosphate-potentiated COI1-JAZ co-receptor. *Nature*, **468**, 400–405.

Studholme, D.J., Ibanez, SG., Maclean, D., Dangl, J.L., Chang, J.H. and Rathjen, J.P. (2009) A draft genome sequence and functional screen reveals the repertoire of type III secreted proteins of *Pseudomonas syringae* pathovar *tabaci* 11528. *BMC Genomics*, **10**, 395.

Turner, J.G. and Novacky, A. (1974) The quantitative relation between plant and bacterial cells involved in the hypersensitive reaction. *Phytopathology*, **64**, 885–890.

Uppalapati, S.R., Ayoubi, P., Weng, H., Palmer, D.A., Mitchell, R.E., Jones, W. and Bender, C.L. (2005) The phytotoxin coronatine and methyl jasmonate impact multiple phytohormone pathways in tomato. *Plant J.* **42**, 201–217.

Uppalapati, S.R., Ishiga, Y., Wangdi, T., Kunkel, B.N., Anand, A., Mysore, K.S. and Bender, C.L. (2007) The phytotoxin coronatine contributes to pathogen fitness and is required for suppression of salicylic acid accumulation in tomato inoculated with *Pseudomonas syringae* pv. *tomato* DC3000. *Mol. Plant–Microbe Interact.* **20**, 955–965.

Wei, C.-F., Kvitko, B.H., Shimizu, R., Crabill, E., Alfano, J.R., Lin, N.-C., Martin, G.B., Huang, H.-C. and Collmer, A. (2007) A *Pseudomonas syringae* pv. *tomato* DC3000 mutant lacking the type III effector HopQ1–1 is able to cause disease in the model plant *Nicotiana benthamiana*. *Plant J.* **51**, 32–46.

Wei, H.-L., Chakravarthy, S., Mathieu, J., Helmann, T.C., Stodghill, P., Swingle, B., Martin, G.B. and Collmer, A. (2015) *Pseudomonas syringae* pv. *tomato* DC3000 type III secretion effector polymutants reveal an interplay between HopAD1 and AvrPtoB. *Cell Host Microbe*, **17**, 752–762.

Worley, J.N., Russell, A.B., Wexler, A.G., Bronstein, P.A., Kvitko, B.H., Krasnoff, S.B., Munkvold, K.R., Swingle, B., Gibson, D.M. and Collmer, A. (2013) *Pseudomonas syringae* pv. tomato DC3000 CmaL (PSPTO4723), a DUF1330 family member, is needed to produce L-*allo*-isoleucine, a precursor for the phytotoxin coronatine. *J. Bacteriol.* **195**, 287–296.

Xin, X.F. and He, S.Y. (2013) *Pseudomonas syringae* pv. *tomato* DC3000: a model pathogen for probing disease susceptibility and hormone signaling in plants. *Annu. Rev. Phytopathol.* **51**, 473–498.

Xin, X.F., Nomura, K., Aung, K., Velasquez, A.C., Yao, J., Boutrot, F., Chang, J.H., Zipfel, C. and He, S.Y. (2016) Bacteria establish an aqueous living space in plants crucial for virulence. *Nature*, **539**, 524–529.

Young, J.M. (1974) Development of bacterial populations in vivo in relation to plant pathogenicity. *NZ. J. Agric. Res.* **17**, 105–113.

Zeng, W. and He, S.Y. (2010) A prominent role of the flagellin receptor FLAGELLIN-SENSING2 in mediating stomatal response to *Pseudomonas syringae* pv *tomato* DC3000 in Arabidopsis. *Plant Physiol.* **153**, 1188–1198.

Zeng, W., Brutus, A., Kremer, J.M., Withers, J.C., Gao, X., Jones, A.D. and He, S.Y. (2011) A genetic screen reveals Arabidopsis stomatal and/or apoplastic defenses against *Pseudomonas syringae* pv. *tomato* DC3000. *PLoS Pathog.* **7**, e1002291.

Zheng, X.Y., Spivey, N.W., Zeng, W., Liu, P.P., Fu, Z.Q., Klessig, D.F., He, S.Y. and Dong, X. (2012) Coronatine promotes *Pseudomonas syringae* virulence in plants by activating a signaling cascade that inhibits salicylic acid accumulation. *Cell Host Microbe*, **11**, 587–596.

SUPPORTING INFORMATION

Additional Supporting Information may be found in the online version of this article at the publisher's website:

Fig. S1 Symptoms in whole *Nicotiana benthamiana* plants at 7 days after dip inoculation with *Pseudomonas syringae* pv. *tomato* (*Pto*) DC3000 and D28E derivatives. The test strains were D29E+*cmaL*, D28E+*cmaL*, D28E T3SS$^-$+*cmaL*, *Pto* DC3000 T3SS$^-$, *Pto* DC3000 T3SS$^-$ Δ*cmaL* and D28E+2+*cmaL*.

Fig. S2 Symptoms in whole *Nicotiana benthamiana* plants at 7 days after dip inoculation with D28E+8 strains differentially producing coronafacic acid (CFA).

Fig. S3 Populations of D28E+2 and D28E+2+*cmaL* at 1, 2 and 4 days after dip inoculation at 10^5 colony-forming units (CFU)/mL corroborate the lack of any significant impact on bacterial growth in *Nicotiana benthamiana* conferred by *cmaL*.

Fig. S4 Additional confocal microscopy images of colony development at 5 days after dip inoculation with 1 : 1 mixtures of D28E+2+*cmaL* labelled with mCherry and D28E+2 labelled with yellow fluorescent protein (YFP).

Fig. S5 Configuration used for leaf image analysis on the Costanza plugin of ImageJ.

Table S1 *Escherichia coli* strains and plasmids used in this study.

Table S2 List of oligonucleotide primers used in this study.

Methods S1 DNA manipulations and plasmid strain constructions.